

Shear thickening in granular suspensions: Interparticle friction and dynamically correlated clusters

Claus Heussinger

Institute for Theoretical Physics, Georg-August University of Göttingen, Friedrich-Hund Platz 1, 37077 Göttingen, Germany

(Received 9 July 2013; published 14 November 2013)

We consider the shear rheology of concentrated suspensions of non-Brownian frictional particles. The key result of our study is the emergence of a pronounced shear-thickening regime, where frictionless particles would normally undergo shear thinning. We can clarify that shear thickening in our simulations is due to enhanced energy dissipation via frictional interparticle forces. Moreover, we evidence the formation of dynamically correlated particle clusters of size ξ , which contribute to shear thickening via an increase in *viscous* dissipation. A scaling argument gives for the associated viscosity $\eta_v \sim \xi^2$, which is in very good agreement with the data.

DOI: [10.1103/PhysRevE.88.050201](https://doi.org/10.1103/PhysRevE.88.050201)

PACS number(s): 45.70.-n, 83.80.Hj, 83.60.Fg, 66.20.Cy

Concentrated suspensions of colloidal particles display interesting non-Newtonian rheological behavior [1]. Shear thickening, i.e., the increase of viscosity with shear rate, is among the most well known effects, and has been studied for many years. In recent years a picture of shear thickening has emerged [2–4] that is based on the notion of hydroclusters, long-lived particle clusters that are stabilized via singular lubrication forces. With confocal imaging techniques it is now possible to visualize these clusters [4], and a quantitative understanding of the connection between cluster formation and shear thickening is within reach.

Another mechanism for shear thickening in dense non-Brownian granular suspensions has been discussed recently in a series of articles [5–8]. The idea is that granular systems dilate, i.e., they want to expand when made to flow. Under conditions of constant volume this leads to an increase in normal stress and, subsequently, an increase in shear resistance. With hydrodynamic thickening leading to a modest viscosity increase, dilation is a huge effect and may effectively jam the suspension into a dynamically arrested state [9,10].

Here, we use computer simulations to study the role of interparticle friction in the shear rheology of dense non-Brownian suspensions. Introducing a particle stiffness k , it is possible to study the transition from the fluid to the plastic flow regime (with a yield stress $\sigma_y \sim k$) by increasing the volume fraction ϕ through the jamming transition at ϕ_c . Several studies are concerned with frictionless particles and scaling laws have been proposed that characterize the jamming transition [11–15]. The main result is that dense frictionless systems generically are shear thinning [11,14]. The role of friction has also been studied in a variety of contexts [16–20] and the most important effect seems to be the mere shift of the critical density to lower values. The exception is the work of Otsuki *et al.* [18], where a discontinuous jump between coexisting fluid and solid branches has been observed. This constitutes the first example of discontinuous shear thickening in a dry *granular powder*.

In the present Rapid Communication on *granular suspensions*, we will recover this discontinuity. What is more intriguing, however, is a second regime of “continuous” shear thickening, which we explain from the enhanced viscous dissipation of dynamically correlated particle clusters.

Model. We consider a two-dimensional ($d = 2$) system of N soft spherical particles. The particle volume (area) fraction is defined as $\phi = \sum_{i=1}^N \pi R_i^2 / L^2$, where L is the size of the

simulation box and R_i is the radius of particle i . To avoid crystallization, we take one half of the particles (“small”) with radius $R_s = 0.5d$, the other half (“large”) with radius $R_l = 0.7d$. Periodic (Lees-Edwards) boundary conditions are used in both directions.

Particles interact via a standard spring-dashpot interaction (similar to, e.g., Refs. [18,19,21]). Two particles i, j interact when they are in contact, i.e., when their mutual distance r is smaller than the sum of their radii $R_i + R_j$. The normal component of the interaction force is $F_n = k_n[r - (R_i + R_j)] - \gamma_n \delta v_n$, where k_n is the spring constant, γ_n the dashpot strength, and δv_n the relative normal velocity of the two contacting particles. The tangential component is $F_t = k_t \delta t$, with δt the tangential (shear) displacement since the formation of the contact. The tangential spring mimics sticking of the two particles due to dry friction. These frictional forces are limited by the Coulomb condition $F_t \leq \mu F_n$, with a constant, i.e., velocity independent friction coefficient μ .

The system is sheared at a shear rate $\dot{\gamma}$. Newton’s equations of motion $m\ddot{\vec{r}}_i = \vec{F}_i^{\text{cont}} + \vec{F}_i^{\text{visc}}$ are integrated with contact forces as specified above and a viscous drag force, which implements the shear flow. The drag force $\vec{F}_i^{\text{visc}}(\vec{v}_i) = -\zeta \delta \vec{v}_i$ is proportional to the velocity difference $\delta \vec{v}_i = \vec{v}_i - \vec{v}_{\text{flow}}$ between the particle velocity \vec{v}_i and the flow velocity $\vec{v}_{\text{flow}}(\vec{r}_i) = \vec{e}_x \dot{\gamma} y$ [11,22–24]. The friction coefficient ζ represents the viscosity of the surrounding fluid, $\zeta \propto \eta_f$. Fluctuations of the flow field as well as hydrodynamic interactions, in particular, lubrication forces, are neglected. Note that this automatically excludes hydrodynamic forces as the possible origin for the shear-thickening phenomena that will be discussed below. In fact, this tailoring of the interaction forces is a key ingredient of our study, because it allows to pinpoint the ultimate cause of the shear thickening in the frictional component.

As units we choose particle mass density ρ , particle diameter d , and the spring constant k_n . With these definitions we perform molecular dynamics simulations using the “Large-scale Atomic/Molecular Massively Parallel Simulator” (LAMMPS) [25] with parameters $\gamma_n = 0.1$, $k_t = 2k_n/7$, a static friction coefficient $\mu = 1$, viscous drag $\zeta = 0.1$, and a time step of $\Delta t = 0.01$. System sizes range from $N = 2500$ to 4900 particles, with a few simulations ranging up to $N = 10\,000$.

The limit $\mu \rightarrow 0$ corresponds to the frictionless scenario, which has been studied, for example, in Refs. [11,12,14]. In these systems jamming is associated with shear-thinning rheology, governed by a critical point at $\phi_c \approx 0.843$ and at

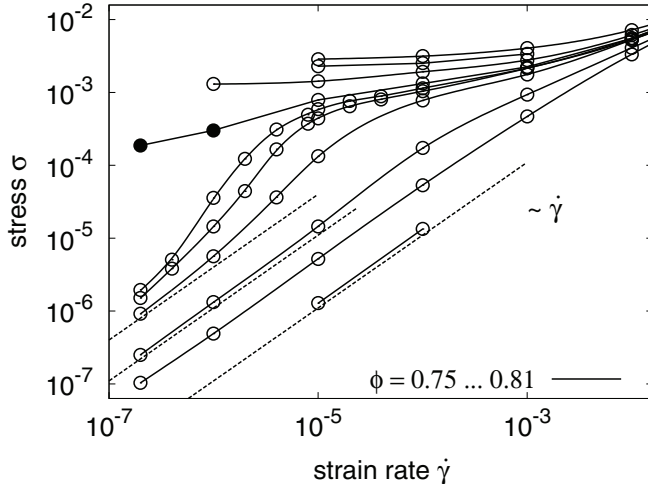


FIG. 1. Flow curves $\sigma(\dot{\gamma})$ for various volume fractions $\phi = 0.75, 0.77, 0.78, 0.79, 0.7925, 0.7935, 0.795, 0.8, 0.805, 0.81$ (from bottom to top).

zero stress, $\sigma_c = 0$. We will show in the following how a simple change to finite and constant friction coefficient $\mu \neq 0$ can fundamentally change this picture.

Results. In Figs. 1 and 2 we display the flow curves and the associated viscosities of our frictional simulations. By varying the volume fraction we go through the jamming transition and observe the associated changes in the flow behavior. At small volume fractions, below the jamming transition, we observe a Newtonian regime $\sigma = \eta_0 \dot{\gamma}$, with a strain-rate-independent viscosity $\eta_0(\phi)$ that increases with volume fraction. At high densities, above jamming, the stress levels off at the yield stress, $\sigma_y(\phi) = \sigma(\dot{\gamma} \rightarrow 0, \phi)$.

In frictionless systems the jamming transition is associated with “critical” shear thinning $\sigma \sim \dot{\gamma}^x$ ($x < 1$, power-law fluid) [11, 12, 14]. Here, surprisingly, the opposite is happening: Jamming is signalled by a shear-thickening regime that grows stronger with increasing the volume fraction. At $\phi = 0.78$ only a mild increase of the viscosity is observed, before it drops in

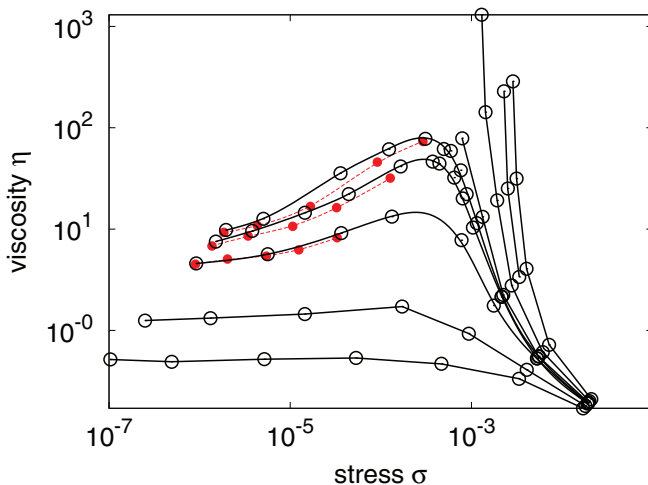


FIG. 2. (Color online) Viscosity $\eta = \sigma/\dot{\gamma}$ vs stress σ for various volume fractions $\phi = 0.77 \dots 0.81$ ($N = 4900$). As a comparison the data from the $N = 10000$ system are given with small (red) symbols.

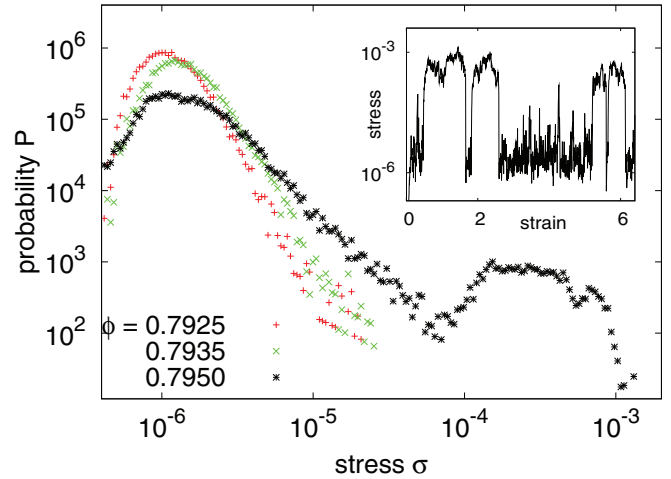


FIG. 3. (Color online) Probability distribution of stress values for different volume fractions ϕ and for $\dot{\gamma} = 2 \times 10^{-7}$. The double-peak structure (for $\phi = 0.795$) indicates the coexistence of jammed and viscous flow regimes. Inset: Stress-strain relation in the coexisting state.

the shear-thinning regime. At $\phi = 0.7935$ the viscosity already increases by about an order of magnitude.

The stress scale in the thickening regime (as characterized, for example, by the stress at the viscosity maximum) is nearly independent of volume fraction. By way of contrast, the strain rate for the onset of thickening decreases with volume fraction (the thickening regime shifts to the left in Fig. 1). This shift does not go down to $\dot{\gamma} \rightarrow 0$. Rather, at about $\phi = 0.795$, the solid data points in Fig. 1 indicate qualitatively different behavior: the *coexistence* of jammed solid and freely flowing fluid states. This is evidenced in Fig. 3. For the solid data points the stress distribution is bimodal (black star) and the stress-strain relation shows sudden switching events from low-stress (fluid) to high-stress (solid) states. By way of contrast, in the (continuous) thickening regime (red plus, green cross) the stress distributions have only one peak. As can be seen in the figure, the tails of this distribution are rather broad, indicative of giant stress fluctuations.

Discussion. The observed phenomena are strongly reminiscent of critical behavior. The coexistence of flowing and jammed states then signals a discontinuous jamming transition (similar to the dry granular flow of Ref. [18]). The coexistence region seems to be terminated by a “critical point” at a certain (nonzero) value of stress, an associated strain rate, and a volume fraction ($\sigma_c, \dot{\gamma}_c, \phi_c$), at which the transition is continuous. The shear-thickening regime then corresponds to the near-critical “isochores” close to but above this point.

Evidence of this scenario of a finite-stress critical point is provided by the fact that stress fluctuations in the shear-thickening regime are strongly enhanced. Equally important, a large correlation length indicates cooperative behavior. To extract such a length scale we calculate the velocity correlation function $C_v(x) = \langle v_y(x)v_y(0) \rangle$, where we concentrate on the velocity component in the gradient direction v_y of two particles separated by x in the flow direction. In the frictionless system this correlation function has been used to evidence a correlation

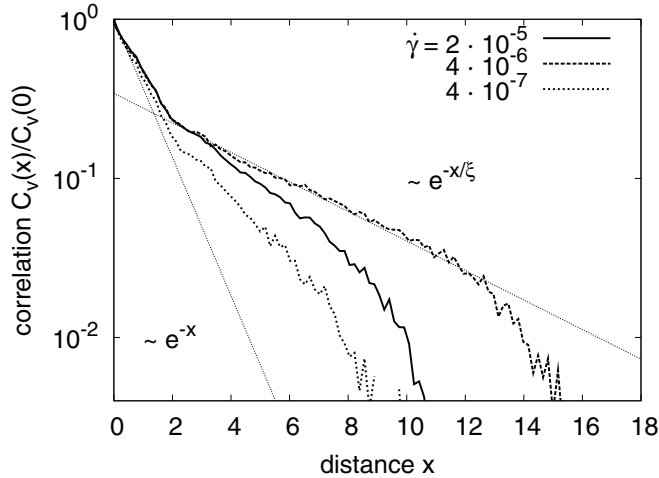


FIG. 4. Velocity correlation function $C_v(x) = \langle v_y(x)v_y(0) \rangle$ for different strain rates and $\phi = 0.7935$.

length that diverges in the limits $\phi \rightarrow \phi_c \approx 0.843$ and $\sigma \rightarrow \sigma_c \equiv 0$ [11,13].

Figure 4 displays the normalized correlation function for $\phi = 0.7935$ and a selected set of strain rates. Beyond a short-range exponential decay, $C_v(x) \sim \exp(-x)$, there is clear nonmonotonic behavior with strain rate $\dot{\gamma}$, indicating a maximal correlation range at some finite value $\dot{\gamma}_c$. This observation can be quantified by defining the length scale ξ from fitting a second exponential, $C_v \sim \exp(-x/\xi)$, as indicated in the figure.¹

The resulting correlation length is displayed in Fig. 5. It clearly shows nonmonotonic behavior both in strain rate $\dot{\gamma}$ and in volume fraction ϕ . The position of the absolute maximum is estimated to be at $\phi_c \approx 0.795$, $\dot{\gamma}_c \approx 2 \times 10^{-6}$, $\sigma_c \approx 10^{-4}$,

¹We have checked that alternative definitions for the length scale ξ do not change the resulting picture.

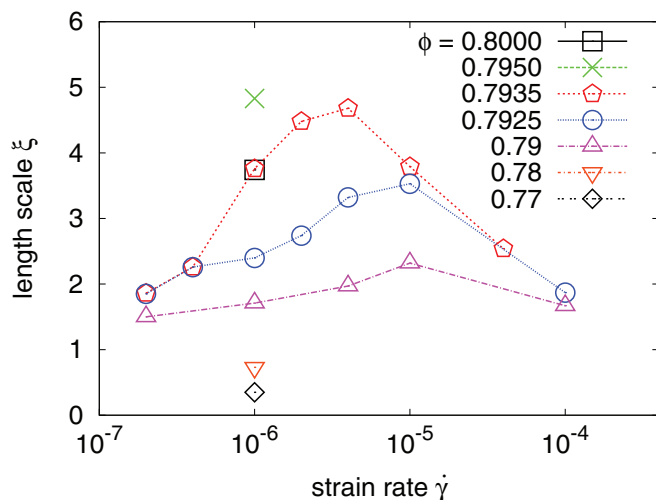


FIG. 5. (Color online) Correlation length as extracted from the exponential fit to $C_v(x)$ for different volume fractions and strain rates.

which may serve as a first proxy to the critical point (see below for further discussion).

Note that in the frictionless scenario of Ref. [11] the correlation length is defined from the minimum of $C_v(x)$. We also observe a minimum, and its behavior is similar to the ξ we define. However, finite-size effects due to the periodic boundary conditions are much stronger and prohibit a quantitative evaluation.

Relation to experiment. The phenomenology described here is remarkably similar to the experiments of Lootens *et al.* [9,10] as well as those of Brown *et al.* [6] and Fall *et al.* [7]. As in the experiments we observe giant stress fluctuations in the thickening regime, as well as the coexistence of flowing and jammed states. Moreover, as in the experiments the normal stress p is tightly coupled to the shear stress σ , such that the effective friction coefficient $\mu = \sigma/p$ is constant (≈ 0.3) throughout the thickening regime (not shown). Thus, it seems that dilatancy effects are at the origin of the shear-thickening regime.

Unlike the experiments of Brown and Fall, however, we do not observe shear localization. Our system is homogeneous and the flow profile is linear. Furthermore, a tight coupling between shear and normal stresses is also observed in simulations of frictionless particles, with either Newtonian or even shear-thinning behavior [26–28]. Therefore, beyond enhanced normal stresses one has to allow for a new channel of energy dissipation via frictional particle interactions. Such a channel is absent in frictionless systems.

In Fig. 6 (inset) we compare the work performed by the external forces ($W = L^2 \eta \dot{\gamma}^2$) with the energy dissipated by the viscous forces ($\Gamma = -\zeta N \langle \delta v^2 \rangle$). Without friction, both should be equal to each other, so that the difference is due to energy dissipation via friction. We see that, indeed, the shear-thickening regime corresponds to an enhanced frictional contribution to energy dissipation. However, and perhaps surprising, even the pure viscous forces do show some thickening behavior.

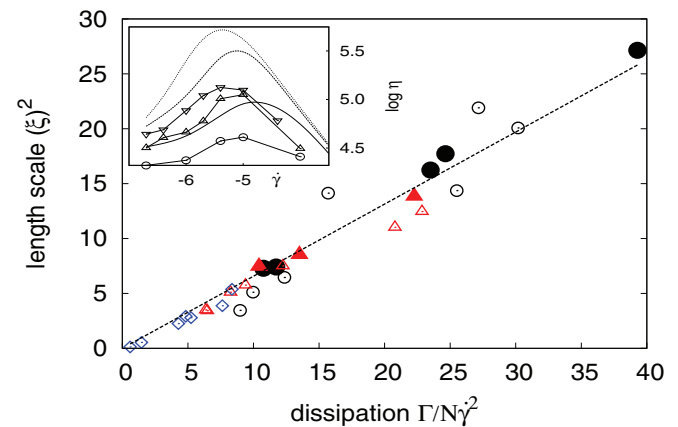


FIG. 6. (Color online) Inset: Comparison of viscosity (logarithmic y axis) as taken from Fig. 1 (thin lines) and as determined from the viscous dissipation $\Gamma/\dot{\gamma}^2$ (symbols). Main panel: Scatter plot of viscous dissipation $\Gamma/N\dot{\gamma}^2$ vs correlation length ξ^2 (circles $\phi = 0.7935$, triangles 0.7925, diamonds 0.770...0.790; small open symbols $N = 4900$, large solid symbols $N = 6400 \dots 8100$). There is a clear linear relation, indicating $\Gamma \propto N\dot{\gamma}^2\xi(\dot{\gamma})^2$.

To explain this latter contribution, we need to remember that shear thickening in our system is tightly connected to the growth of a correlation length. If particles move in correlated clusters of size ξ , then the typical velocity scales as $\delta v \sim \dot{\gamma} \xi$. This leads to a renormalized energy dissipation $\Gamma \sim \dot{\gamma}^2 \xi^2$ and associated viscosity $\eta_v(\dot{\gamma}) \sim \xi(\dot{\gamma})^2$. This relation is plotted in the main panel of Fig. 6. It holds remarkably well with a prefactor of order unity.

A similar argument holds in frictionless systems [29,30], where the relation between correlation length, and velocity fluctuations can be used to rationalize the divergence of the (Newtonian) viscosity with increasing the volume fraction towards the close packing limit, $\eta(\phi) \sim \xi(\phi)^2$. In this picture, the viscosity diverges at close packing because of the growth of dynamically correlated particle clusters and an associated divergence of velocity fluctuations [29,30].

With the equivalence between correlation length and viscosity η_v , we have to reconsider the nature and location of the critical point. A divergence of the correlation length should be equally visible as divergence in the viscosity. However, as discussed in Ref. [6], the shear-thickening regime is limited from above by an appropriate energy scale which represents the softest link in the system (there, surface tension of the air-fluid interface). The viscosity can therefore not grow beyond this scale. In our system this energy scale is played by the stiffness k_n of the particles. When the viscosity $\eta_v \sim \zeta \xi^2$ of the thickening fluid is comparable to the yield stress $\sigma \sim k_n$ in the plastic flow regime, then thickening stops. For the critical

point, this means that it may be hidden within the plastic flow regime. Hard-sphere simulations, similar to Ref. [15], could give valuable information in this regard.

In conclusion, we discuss the shear rheology of a non-Brownian suspension of soft spherical particles. Hydrodynamic interactions are neglected and we concentrate on the effects of frictional particle interactions, characterized by a constant friction coefficient μ . This tailoring of the interaction forces is a key advantage of our study. With this we can show that friction does indeed lead to pronounced shear thickening, unlike in frictionless systems which are shear thinning. Friction is therefore an essential ingredient for the thickening behavior observed. Note that similar shear-thickening phenomena with more complex interaction forces have been presented just recently in Refs. [31,32]. Going beyond these studies we observe giant stress fluctuations and a growing correlation length, which is maximal deep within the thickening regime. We show that thickening is partly due to enhanced energy dissipation via frictional interactions. In addition, dynamically correlated clusters of size ξ also lead to an increased *viscous* contribution to the energy dissipation. A scaling argument gives for the associated viscosity $\eta_v \sim \eta_f \xi^2$, which is in very good agreement with the data.

Acknowledgments. Fruitful discussions with M. Grob and A. Zippelius are acknowledged. Financial support comes from the Deutsche Forschungsgemeinschaft, Emmy Noether Program No. He 6322/1-1.

-
- [1] J. Mewis and N. J. Wagner, *Colloidal Suspension Rheology* (Cambridge University Press, Cambridge, UK, 2011).
- [2] N. J. Wagner and J. F. Brady, *Phys. Today* **62**(10), 27 (2009).
- [3] J. F. Brady and G. Bossis, *J. Fluid Mech.* **155**, 105 (1985).
- [4] X. Cheng, J. H. McCoy, J. N. Israelachvili, and I. Cohen, *Science* **333**, 1276 (2011).
- [5] E. Brown and H. M. Jaeger, *Phys. Rev. Lett.* **103**, 086001 (2009).
- [6] E. Brown and H. Jaeger, *J. Rheol.* **56**, 875 (2012).
- [7] A. Fall, F. Bertrand, G. Ovarlez, and D. Bonn, *J. Rheol.* **56**, 575 (2012).
- [8] A. Fall, N. Huang, F. Bertrand, G. Ovarlez, and D. Bonn, *Phys. Rev. Lett.* **100**, 018301 (2008).
- [9] D. Lootens, H. van Damme, Y. Hémar, and P. Hébraud, *Phys. Rev. Lett.* **95**, 268302 (2005).
- [10] D. Lootens, H. Van Damme, and P. Hébraud, *Phys. Rev. Lett.* **90**, 178301 (2003).
- [11] P. Olsson and S. Teitel, *Phys. Rev. Lett.* **99**, 178001 (2007).
- [12] B. P. Tighe, E. Woldhuis, J. J. C. Remmers, W. van Saarloos, and M. van Hecke, *Phys. Rev. Lett.* **105**, 088303 (2010).
- [13] C. Heussinger and J.-L. Barrat, *Phys. Rev. Lett.* **102**, 218303 (2009).
- [14] M. Otsuki and H. Hayakawa, *Phys. Rev. E* **80**, 011308 (2009).
- [15] E. Lerner, G. Düring, and M. Wyart, *Proc. Natl. Acad. Sci. USA* **109**, 4798 (2012).
- [16] F. da Cruz, S. Emam, M. Prochnow, J.-N. Roux, and F. Chevoir, *Phys. Rev. E* **72**, 021309 (2005).
- [17] M. Trulsson, B. Andreotti, and P. Claudin, *Phys. Rev. Lett.* **109**, 118305 (2012).
- [18] M. Otsuki and H. Hayakawa, *Phys. Rev. E* **83**, 051301 (2011).
- [19] M. P. Ciamarra, R. Pastore, M. Nicodemi, and A. Coniglio, *Phys. Rev. E* **84**, 041308 (2011).
- [20] S. Chialvo, J. Sun, and S. Sundaresan, *Phys. Rev. E* **85**, 021305 (2012).
- [21] L. E. Silbert, D. Ertas, G. S. Grest, T. C. Halsey, and D. Levine, *Phys. Rev. E* **65**, 031304 (2002).
- [22] D. J. Durian, *Phys. Rev. Lett.* **75**, 4780 (1995).
- [23] A. Scala, T. Voigtmann, and C. D. Michele, *J. Chem. Phys.* **126**, 134109 (2007).
- [24] B. Lander, U. Seifert, and T. Speck, *Europhys. Lett.* **92**, 58001 (2010).
- [25] <http://lammps.sandia.gov/index.html>
- [26] C. Heussinger, P. Chaudhuri, and J.-L. Barrat, *Soft Matter* **6**, 3050 (2010).
- [27] P. Olsson and S. Teitel, *Phys. Rev. E* **83**, 030302 (2011).
- [28] P.-E. Peyneau and J.-N. Roux, *Phys. Rev. E* **78**, 011307 (2008).
- [29] B. Andreotti, J.-L. Barrat, and C. Heussinger, *Phys. Rev. Lett.* **109**, 105901 (2012).
- [30] C. Heussinger, L. Berthier, and J.-L. Barrat, *Europhys. Lett.* **90**, 20005 (2010).
- [31] N. Fernandez, R. Mani, D. Rinaldi, D. Kadau, M. Mosquet, H. Lombois-Burger, J. Cayer-Barrioz, H. J. Herrmann, N. D. Spencer, and L. Isa, *Phys. Rev. Lett.* **111**, 108301 (2013).
- [32] R. Seto, R. Mari, J. F. Morris, and M. M. Denn, arXiv:1306.5985.